Toroidal and poloidal vessel currents during asymmetrical disruptions on COMPASS

E. Matveeva[1,2], J. Havlicek[1], A. Havranek[1], V. Yanovskiy[1],
S.N. Gerasimov[3], V.D. Pustovitov[4,5], O. Hronova[1], V. Weinzettl[1], the COMPASS team[1]

[1] *Institute of Plasma Physics of the CAS, Prague, Czech Republic*

[2] *Charles University, Faculty of Mathematics and Physics, Prague, Czech Republic*

[3] *CCFE, Culham Science Centre, Abingdon, Oxon, OX14 3DB, UK*

[4] *National Research Centre Kurchatov Institute, Moscow, Russia*

[5] *National Research Nuclear University MEPhI, Moscow, Russia*

Introduction

Determination of the vessel currents magnitudes and distributions plays crucial role in understanding of mechanical loads on the machine [1, 2]. For the first time, the plasma current asymmetries and vessel currents along with their poloidal and toroidal distributions are measured simultaneously in the COMPASS tokamak. Experimentally measured poloidal eddy currents exhibit agreement with theoretical predictions [5]. Comparison of toroidal asymmetries of Halo currents and plasma current suggests that part of the plasma current is transferred to the wall in poloidal direction.

Magnetic diagnostics

The COMPASS tokamak has unique magnetic diagnostics (Fig. 1) including full internal and full external Rogowski coils, three sets of Mirnov coils MC (each coil capable of measuring radial, toroidal and poloidal components of magnetic field), internal and external partial Rogowski coils (IPR and EPR). This allows detection of plasma current in 5 toroidal positions and, therefore, study of toroidal asymmetries during disruptions. Toroidal vessel currents are measured using IPR and EPR coils. Both sets are at the same toroidal position and the coils are at the same poloidal angles separated only by 3mm thick vessel wall (Fig. 2). The difference between IPR and EPR signals provides information about poloidal field created by toroidal vessel current. The current magnitude is obtained by the following equation: $J_w = \frac{(B_{IPR}-B_{EPR})2L}{\mu_0}$, where B_{EPR} and B_{IPR} are the local poloidal magnetic field detected by EPR and IPR coils, L is the coil length in poloidal direction and is equal to 4 cm. Poloidal currents in the vessel are proportional to the change in the toroidal magnetic field. According to Ampere's law [6], $I_w = \frac{2\pi R_0}{\mu_0}\Delta B$, where $\Delta B = B_{tor}^{ext} - B_{tor}^{MC}$ is a difference between externally applied toroidal field and a signal collected by individual toroidal Mirnov coil inside the vessel.

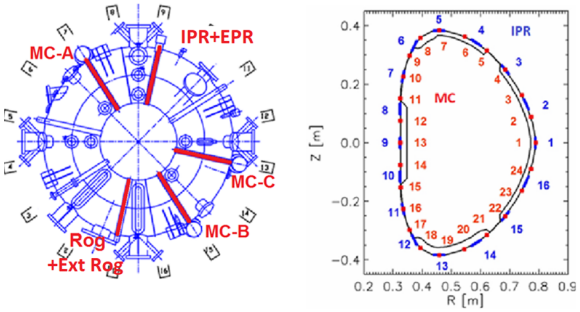

Figure 1: *COMPASS tokamak magnetic diagnostics. 16 Internal partial Rogowski coils (IPR), 16 External partial Rogowski coils (EPR), Rogowski coil (Rog), full external Rogowski coil (Ext Rog), 3 rings of Mirnov coils (72 coils at 24 positions) (MC-A, MC-B, MC-C).*

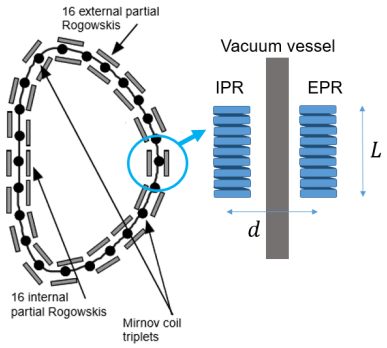

Figure 2: *External and Internal Partial Rogowski coils positions in poloidal cross-section. Each pair at same poloidal angle is separated by 3 mm wall*

Toroidal vessel currents

A typical example of J_w is shown in (Fig. 3a). Disruption starts with plasma vertical movement upwards. Toroidal dipole-like eddy currents are induced in order to counteract this motion reaching its peak of 4 kA at 1085. During current quench starting at 1085.4 ms (CQ) J_w sign reverses in plasma-wall contact region due to I_p loss. Peak value during CQ reaches 12 kA.

Poloidal vessel currents

Poloidal currents I_w during downward disruption are shown in (Fig. 3b). During thermal quench poloidal diamagnetic currents are induced in the vessel. They are symmetrical and do not exceed 3 % of predisruptive plasma current I_p^{disr}. Largest I_w are observed during CQ as Halo region starts to play role. Halo currents are localized in the plasma-wall contact region and reach up to 20 % of I_p^{disr}. Their magnitude increases with I_p^{disr} as shown in (Fig. 4a, top). Halo currents tend to be largest for fastest disruptions (Fig. 4a, bottom). This opposes JET data [4], but is consistent with NSTX measurements [3]. NSTX and COMPASS both often exhibit significant vertical motion prior thermal and current quenches and large Halo current is generated. On the other hand JET vertical displacement occurs at reduced I_p leading to smaller Halo currents. Halo currents and I_p difference between two opposite toroidal positions are in counter-phase indicating that part of the plasma toroidal current is transferred to the wall in poloidal direction (Fig. 4b).

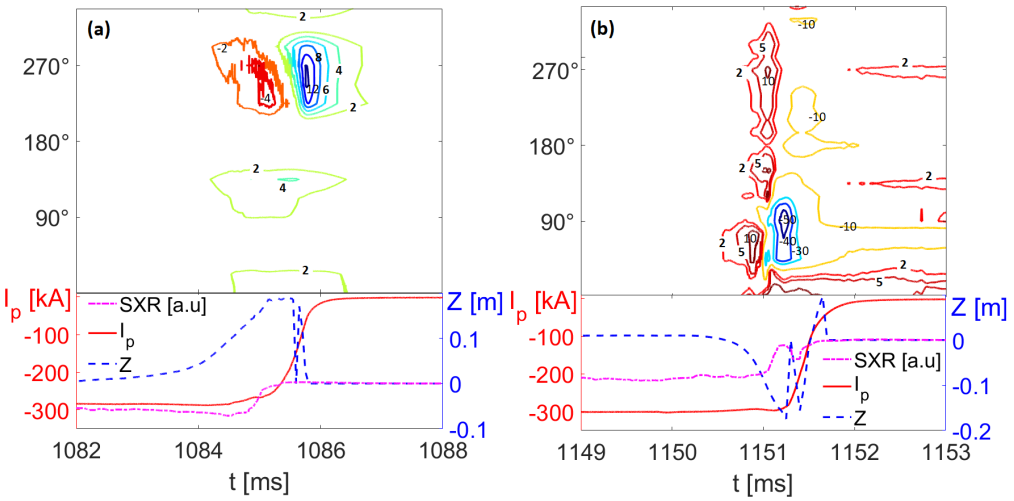

Figure 3: *Contour plots of the vessel currents. Each curve represents isoline of the vessel currents. Poloidal angle is counted from the low field side midplane counterclockwise. (a) Top: toroidal vessel currents for upward disruption in kA/4cm #10674. J_w distribution as a function of time and poloidal angle. Dipole-like current is observed at 1085 ms. Current spike up to 12 kA appears at 1086.5 ms in the region of plasma-wall contact (b) Top: poloidal vessel currents for downward disruption #18770. I_w distribution as a function of time and poloidal angle. Symmetric current up to 5 kA is observed at 1151 ms followed by Halo currents up to -50 kA. Bottom (a,b): time evolution of I_p, vertical position and SXR (drop indicates thermal quench)*

Analytical estimation of eddy currents

Theoretical relation between poloidal eddy currents in the vessel and plasma parameters based on flux-conserving plasma equilibrium has been presented in [5]. The current in the wall is derived as follows:

$$L_w \frac{dI_w}{dt} + R_w I_w + \frac{\Phi_{pl} - \Phi_{pl}^0}{dt} + L_w \frac{dI_{tc}}{dt} = 0, \tag{1}$$

where $\Phi_{pl} - \Phi_{pl}^0 \approx \frac{2K}{K^2+1} \frac{(I_{pl}\mu_0)^2}{8\pi B_0}$, K is the plasma elongation, L_w is the poloidal inductance, I_{tc} is the full poloidal current in toroidal coils, B_0 is the toroidal field, I_{pl} is the plasma current. In the ideal wall case, the second and forth terms of Eqn. (1) vanish.

For preliminary validation of this theoretical estimation toroidal Mirnov coil #8 data is investigated for 27 downward disruptions. Coil #8 is located in the top of the vessel and measures primarily poloidal eddy currents, while Halo currents are concentrated in the bottom. Peak eddy current during thermal quench is determined and compared to analytical predictions. These values are in good agreement with Eqn. (1) (ideal wall) for highest plasma currents (up to 13% difference between predicted and measured values). However, there is significant discrepancy observed for discharges with lower plasma current. This might be due to the fact that eddy cur-

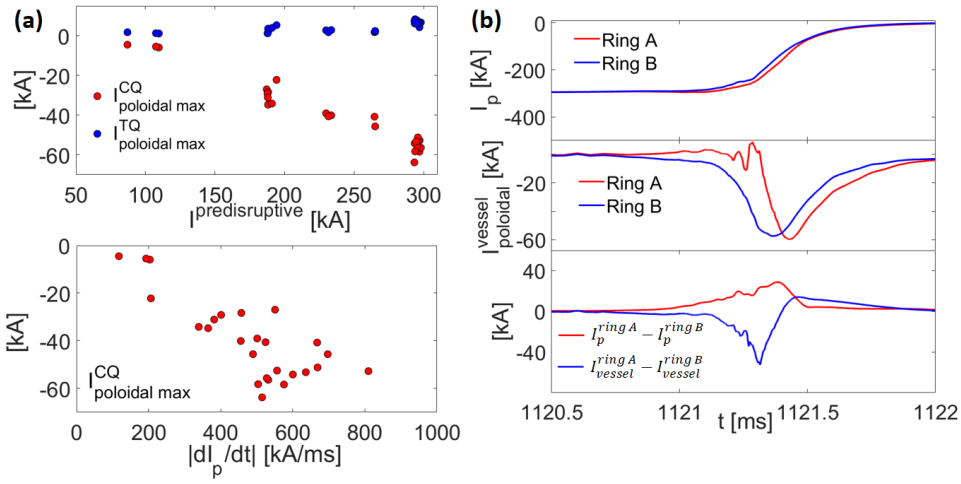

Figure 4: *(a) Peak poloidal currents. Top: peak Halo currents (blue dots) and eddy currents during TQ dependence on predisruptive plasma current. Bottom: peak Halo currents plotted against current quench velocity. (b) Halo current asymmetry for downward disruption # 18765 measured by bottom MC #18 (detects primarily Halo current). Top: I_p in two opposite toroidal positions (A and B). Middle: Poloidal vessel currents. Bottom: I_p and vessel currents difference between two opposite toroidal positions.*

rents are relatively small (3 % of I_p^{disr}) and toroidal Mirnov coil signal is too weak for accurate measurements.

Conclusions

Non-symmetric structure of poloidal and toroidal vessel currents during disruptions has been illustrated by experimental data. Observed poloidal eddy currents are consistent with theory, but future systematic investigation of resistive wall case is needed. Plasma current and Halo currents toroidal asymmetry during disruptions exhibit counter phase behavior.

Acknowledgment

This work has been carried out within the framework of the EUROfusion Consortium and has received funding from the Euratom research and training programme 2014-2018 and 2019-2020 under grant agreement No 633053. The views and opinions expressed herein do not necessarily reflect those of the European Commission. Co-funded by MEYS project number 8D15001. Co-funded by MEYS project LM2015045.

References

[1] S.N. Gerasimov et al., *37th EPS Conference on Plasma Physics*, 1206 (2010)

[2] S.N. Gerasimov et al., *Nucl. Fusion*, **54**, 113006 (2014)

[3] S.P. Gerhardt et al. *Nucl. Fusion*, **52**, 063005 (2012)

[4] V. Riccardo et al., *Plasma Physics and Controlled Fusion* , **46**, 925 (2004)

[5] V.D. Pustovitov, *Fusion Engineering and Design* , **117**, 1-7 (2017)

[6] P.J. Knight et al., *Nuclear Fusion* , **40**, 325 (2000)